White Matter Degeneration Pathways Associated With Tau Deposition in Alzheimer Disease

Jianqiao Tian, MS, Sheelakumari Raghavan, PhD, Robert I. Reid, PhD, Scott A. Przybelski, BS,
Timothy G. Lesnick, MS, Robel K. Gebre, PhD, Jonathan Graff-Radford, MD, Christopher G. Schwarz, PhD,
Val J. Lowe, MD, Kejal Kantarci, MD, David S. Knopman, MD, Ronald C. Petersen, MD, PhD,
Clifford R. Jack, Jr., MD, and Prashanthi Vemuri, PhD

Correspondence
Dr. Vemuri
vemuri.prashanthi@
mayo.edu

Abstract

Background and Objectives
The dynamics of white matter (WM) changes are understudied in Alzheimer disease (AD). Our goal was to study the association between flortaucipir PET and WM health using neurite orientation dispersion and density imaging (NODDI) and evaluate its association with cognitive performance. Specifically, we focused on NODDI's Neurite Density Index (NDI), which aids in capturing axonal degeneration in WM and has greater specificity than single-shell diffusion MRI methods.

Method
We estimated regional flortaucipir PET standard uptake value ratios (SUVRs) from 3 regions corresponding to Braak stage I, III/IV, and V/VI to capture the spatial distribution pattern of the 3R/4R tau in AD. Then, we evaluated the associations between these measurements and NDIs in 29 candidate WM tracts using Pearson correlation and multiple regression models.

Results
Based on 223 participants who were amyloid positive (mean age of 78 years and 57.0% male, 119 cognitively unimpaired, 56 mild cognitive impairment, and 48 dementia), the results showed that WM tracts NDI decreased with increasing regional Braak tau SUVRs. Of all the significant WM tracts, the uncinate fasciculus ($r = -0.274$ for Braak I, -0.311 for Braak III/IV, and -0.292 for Braak V/VI, $p < 0.05$) and cingulum adjoining hippocampus ($r = -0.274$, -0.288, -0.233, $p < 0.05$), both tracts anatomically connected to areas of early tau deposition, were consistently found to be within the top 5 distinguishing WM tracts associated with flortaucipir SUVRs. The increase in tau deposition measurable outside the medial temporal lobes in Braak III–VI was associated with a decrease in NDI in the middle and inferior temporal WM tracts. For cognitive performance, WM NDI had similar coefficients of determination ($r^2 = 31\%$) as regional Braak flortaucipir SUVRs (29%), and together WM NDI and regional Braak flortaucipir SUVRs explained 46% of the variance in cognitive performance.

Discussion
We found spatially dependent WM degeneration associated with regional flortaucipir SUVRs in Braak stages, suggesting a spatial pattern in WM damage. NDI, a specific marker of axonal density, provides complementary information about disease staging and progression in addition to tau deposition. Measurements of WM changes are important for the mechanistic understanding of multifactorial pathways through which AD causes cognitive dysfunction.

Glossary

Aβ = β-amyloid; **AD** = Alzheimer disease; **ADRC** = Alzheimer's Disease Research Center; **CGH** = cingulum adjoining hippocampus; **CU** = cognitively unimpaired; **dMRI** = diffusion MRI; **DTI** = diffusion tensor imaging; **GM** = gray matter; **ISOVF** = isotropic volume fraction; **ITWM** = inferior temporal WM; **LASSO** = least absolute shrinkage and selection operator; **MCI** = mild cognitive impairment; **MCSA** = Mayo Clinic Study of Aging; **MMSE** = Mini-Mental State Examination; **MTWM** = middle temporal WM; **NDI** = neurite density index; **NODDI** = neurite orientation dispersion and density imaging; **ODI** = orientation dispersion index; **PiB** = Pittsburgh compound B; **ROI** = region of interest; **SUVR** = standard uptake value ratio; **UNC** = uncinate fasciculus; **WM** = white matter.

Cerebral white matter (WM) plays a central role in the brain's cognitive function by acting as the connectivity infrastructure of the cerebral cortex. However, WM changes in Alzheimer disease (AD) are not as well understood as gray matter (GM), because GM is the site of primary AD pathologic changes, specifically, deposition of hyperphosphorylated tau and amyloid-beta peptide. On the other hand, evidence from structural and functional connectivity studies indicates that WM integrity is key for efficient cognitive functioning[1,2] and suggests that understanding WM integrity changes as a function of aging and age-related pathologies such as AD can provide insights into disease processes.[3,4]

Advances in diffusion MRI (dMRI), particularly those incorporating multishell dMRI techniques, such as neurite orientation dispersion and density imaging (NODDI), enable us to capture subvoxel tissue-specific microstructural properties. Traditionally, diffusion tensor imaging (DTI) has been the most widely available and used dMRI model to study brain microstructure in vivo. Although DTI can be fit using single-shell dMRI, it cannot handle the multiple diffusion environments that typically exist in any given voxel, creating problems for specificity and interpretability. Newer multishell MRI acquisitions support more appropriate modeling (such as NODDI). NODDI models the voxel contents as neurites (thin pipes and nominally axons), the spaces between them, and freely diffusing water (CSF and/or interstitial fluid). It provides 3 separate measures: (1) neurite density index (NDI, a proxy for axonal density), (2) orientation dispersion index (ODI), and (3) isotropic volume fraction (ISOVF, the fraction of water in the voxel that is freely diffusing). All are dimensionless values from 0 to 1, and ODI is 0 for completely parallel neurites and 1 for isotropically distributed neurites.[5] Both DTI and advanced dMRI studies coupled with pathology studies have helped us better understand WM changes due to increased tau burden. Postmortem study evidence suggests that there is a complex interplay between the degeneration of fiber pathways and cortical tau pathology[6] and the earlier changes to the WM microstructure[7] in AD. Previous studies also provided in vivo evidence of the spread of tau pathology through structurally connected brain regions obtained by dMRI in cognitively normal individuals, typical AD, and pathologically staged AD.[8-10] Moreover, a recent study showed a negative association between WM connectivity and tau PET measurements in the early Braak regions[11]

and suggested the synergistic effect of tau and dysconnectivity on neurocognitive performance. Interestingly, AD mouse models showed reduced NDI in WM, which correlated with histologically measured tau protein levels.[12] Furthermore, reduced cortical and WM NDI has been found in association with tau pathology in mild cognitive impairment (MCI) and AD.[13-15] However, the association patterns differed between studies, and the stepwise progressive involvement of WM tracts as a function of disease progression and its relevance to cognitive performance remains unclear. Evidence also suggested that impaired cognition could result from both declining WM connectivity and increasing tau deposition.[11] In this context, Braak staging model reflects early, intermediate, and later stages of the tau deposition[16] measurable in vivo using recently developed tau PET methods and can be specifically used for investigating these underexplored associations between tau deposition and WM damage.

The overarching hypothesis of our work was that there would be significant WM damage local to the regional tau deposition that would be a contributor to poor cognition, and NDI from NODDI can help capture this WM damage. To test this hypothesis, our primary aim was to identify and quantify the extent of WM damage by NDI throughout the brain as a function of the flortaucipir PET signal in the regions featured in Braak stages. The secondary aim was to evaluate the clinical relevance of the WM changes to cognitive performance. For this work, we identified individuals along the AD continuum from the population-based sample of Mayo Clinic Study of Aging (MCSA) and clinically referred participants from Mayo Alzheimer's Disease Research Center (ADRC).

Methods

Selection of Participants

This current study included participants from 2 data sets, which are, MCSA and ADRC. The inclusion criteria included usable β-amyloid (Aβ)-PET, Flortaucipir-PET, multishell dMRI (NODDI), and complete cognitive assessments. Given the widespread evidence that tau deposition is significant and spreads out of the medial temporal lobe because of the presence of amyloidosis, we limited this study to Aβ+ participants to generate a more characteristic spatial distribution pattern of tau deposition seen in the late-onset AD.[17] We

Figure 1 NDI at Each Significant ROI
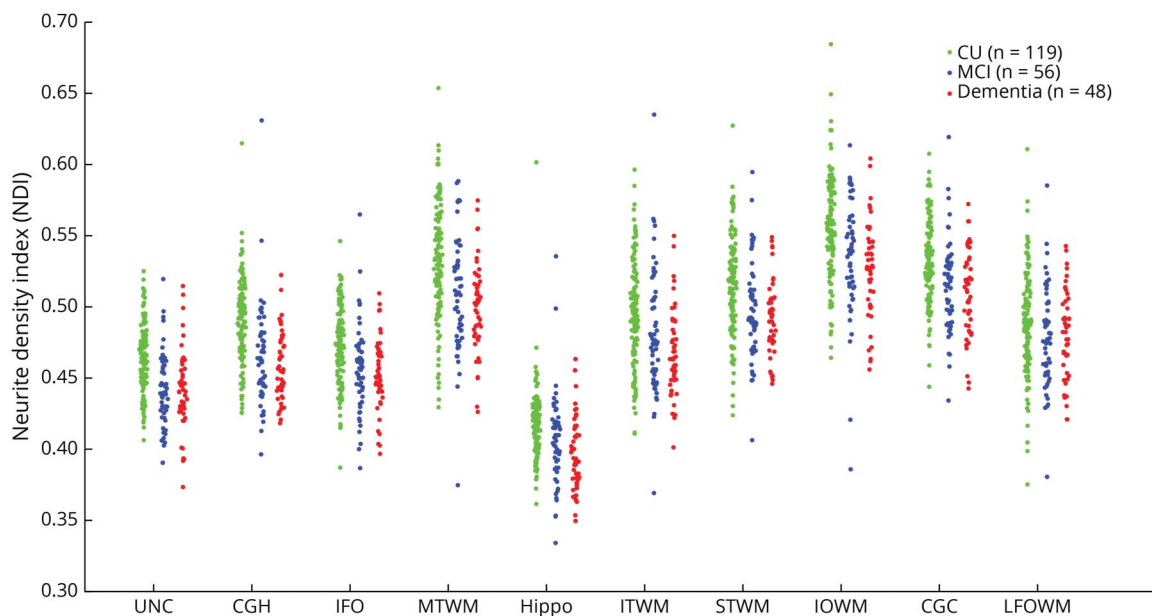
These ROIs were the WM tracts that showed a significant correlation with flortaucipir SUVRs. Note that the NDI difference is more distinctive between CU and the other 2 groups, indicating NDI can be an early detectable change associated with AD-caused cognitive impairment. The full list of the ROIs and their abbreviation definition can be found in eTable 1 (links.lww.com/WNL/C742). AD = Alzheimer disease; CGC = cingulum; CGH = cingulum adjoining hippocampus; CU = cognitively unimpaired; Hippo = hippocampus; IFO = inferior fronto-occipital fasciculus; IOWM = inferior occipital WM; ITWM = inferior temporal WM; LFOWM = lateral fronto-orbital WM; MCI = mild cognitive impairment; MTWM = middle temporal WM; NDI = neurite density index; ROI = region of interest; STWM = superior temporal WM; SUVR = standard uptake value ratio; WM = white matter.

further limited dementia participants in ADRC to be older than 65 years.

MCSA Participants

MCSA is a prospective population-based study cohort that was designed to investigate the incidence and prevalence of MCI and dementia among the residents of Olmsted County, MN.[18] The Olmsted County population was enumerated using the Rochester Epidemiology Project medical records-linkage system in 2004.[19] Participants underwent detailed clinical evaluation, including neuropsychological evaluation with consistent standards,[20] and participated in imaging scans. All included MCSA participants had Aβ deposition based on a Pittsburgh compound B (PiB)-PET cutoff.

ADRC Participants

From Mayo ADRC, we included patients with clinically diagnosed AD dementia older than 65 years to help focus on late-onset AD (who are more likely to have typical patterns of tau deposition identified by Braak stages).

Standard Protocol Approvals, Registrations, and Patient Consents

The study was reviewed and approved by the Mayo Clinic and Olmsted Medical Center institutional review boards. All participants were provided with written information, and written consent was collected from all participants/caregivers. The basic collected demographic information includes age, biological sex, and years of education.

Imaging

MRI Acquisition and Processing

MRI was acquired on 2 identical 3 T Siemens Prisma scanners with 64-channel receiver coils and multiband capability. All participants underwent the same imaging acquisition protocol.[21] The dMRI processing included denoising,[22] eddy current distortion and head motion correction,[23] Gibbs ringing correction,[24] and Rician debiasing.[25] NODDI estimation (NDI, ODI, and ISOVF) was done using accelerated microstructure imaging using Convex Optimization.[26] The JHU "Eve" WM atlas[27] was warped (FA to FA) to participant native space to generate the regional NODDI measures. In this study, we only focused on NDI as the measurement for WM integrity because we were interested in axonal density changes as a function of tau. Mean NDI measures were computed for 29 WM tracts (eTable 1, links.lww.com/WNL/C742) and then computed the voxel number weighted average of left and right hemispheres for each region of interest (ROI). Figure 1 illustrates the NDI distribution in our cohort, separated into 3 cognitive groups: cognitively unimpaired (CU), MCI, and dementia.

Amyloid and Tau PET Imaging

Amyloid and tau deposition were measured in vivo through PiB PET and flortaucipir PET, respectively. The imaging acquisition and processing procedures were described previously. From PiB PET scans, we extracted the global amyloid standard uptake value ratio (SUVR) by averaging the median

Figure 2 Braak Stage Regions and Corresponding Significant WM Tracts
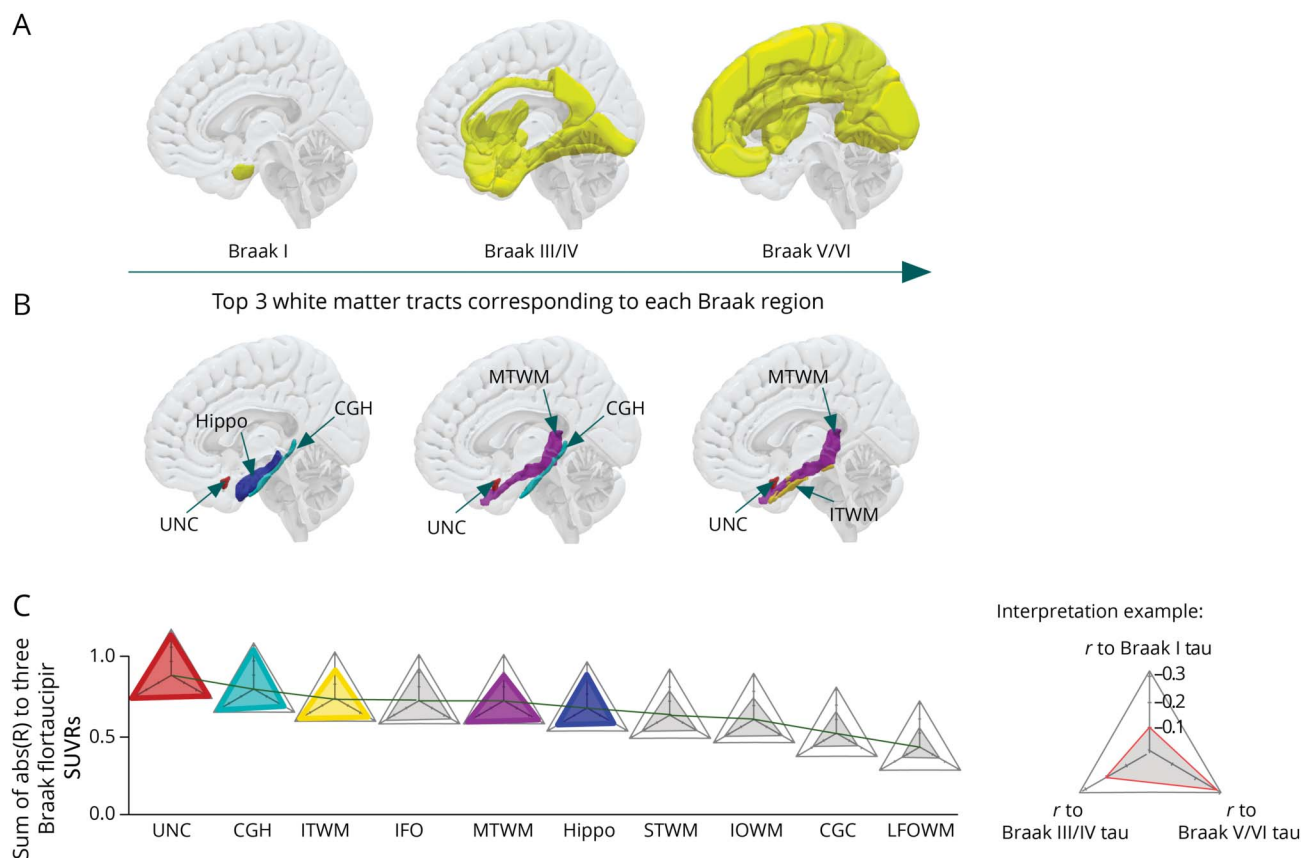
(A) Gray matter regions that have been assigned to each Braak stage. In typical AD, tau protein accumulation has been shown to start from the entorhinal cortex located in the medial temporal lobe and eventually spread to the whole isocortical area. (B) Top 3 WM tracts to each corresponding Braak stage region, ranked by the correlation coefficient. (C) Summary of WM tracts NDI correlation to 3 Braak regions, ranked by their total correlation coefficients to flortaucipir PET SUVRs from all 3 Braak regions. (Interpretation example) Each WM tract was represented by 1 triangular radar symbol. Tract's correlation coefficient to Braak I, Braak III/IV, and Braak V/VI flortaucipir SUVR was represented by the height of each corner. The exemplar triangular figure to the right bottom corner demonstrates a WM track with correlation coefficients of −0.1, −0.2, and −0.3 to Braak I, III/IV, and V/VI flortaucipir SUVR, respectively. The full list of the ROIs and their abbreviation definition can be found in eTable 1 (links.lww.com/WNL/C742). AD = Alzheimer disease; CGC = cingulum; CGH = cingulum adjoining hippocampus; CU = cognitively unimpaired; Hippo = hippocampus; IFO = inferior fronto-occipital fasciculus; IOWM = inferior occipital WM; ITWM = inferior temporal WM; LFOWM = lateral fronto-orbital WM; MTWM = middle temporal WM; ROI = region of interest; STWM = superior temporal WM; SUVR = standard uptake value ratio; WM = white matter.

uptake values in the prefrontal, orbitofrontal, parietal, temporal, anterior cingulate, and posterior cingulate/precuneus regions and then normalizing by the median PiB PET uptake in the cerebellar crus gray matter. We used a previously established amyloid positivity cutoff of SUVR ≥1.48.[28]

To study tau deposition and its correlation to WM integrity changes, we extracted flortaucipir SUVRs at a regional level. Flortaucipir PET images were first registered on our in-house ADIR122 GM atlas (available at nitrc.org/projects/mcalt/), and regional flortaucipir SUVRs were calculated on selected regions that have been recognized as the typical regions for Braak staging. Braak staging model describes the spatial distribution pattern of tau protein with increasing disease severity: transentorhinal cortex (stage I) and hippocampus (stage II), inferior and medial temporal cortex along with posterior cingulum cortex (stage III and IV), and finally, the isocortex of the frontal and parietal lobes (stage V and VI)

which are shown as part of Figure 2A and eTable 2 (links.lww.com/WNL/C743). Specifically in this study, regions that were featured in the same Braak stage were grouped together as Braak regions. They only serve a region map to estimate regional SUVRs, instead of staging criteria. In addition, we did not include the region featured in Braak stage II because of contamination of the choroid plexus signal with the hippocampal tau signal.[29] Figure 3 illustrates flortaucipir SUVRs distribution at 3 Braak regions.

Cognitive Evaluation

All participants underwent a concise cognitive evaluation at the time of image acquisition and were administered the Short Test of Mental Status, which was transformed into Mini-Mental State Examination (MMSE). Short Test of Mental Status is a quick questionnaire for clinical cognitive evaluation that is similar to the commonly used MMSE, and its performance has been clinically validated.[30]

Statistical Analyses

The association between WM integrity and Braak stage was estimated using 2 methods: Pearson correlation coefficient analysis and multiple linear regression analysis. We performed Pearson correlation to separately compute associations between each of the 29 WM NDI measures and flortaucipir PET SUVRs measured at 3 Braak staging regions, as well as with MMSE. These Pearson correlation coefficients were adjusted for age, sex, years of education, and global PiB PET SUVR. A significant issue with solely relying on Pearson correlation coefficients analysis was that correlation analysis separately investigates the association between each WM NDI with the output variable (Braak flortaucipir SUVR) and WM measures in the brain are highly collinear.

We also fit a multiple linear regression model with 29 WM NDIs as the input variables and flortaucipir PET SUVRs from 3 Braak stage regions, or MMSE, as the output. With the multiple linear regression model, we were able to investigate the significance of each WM tract in the progression of tau deposition or cognitive impairment by comparing the weights extracted from the trained multiple linear regression model. To identify the important WM tracts to AD staging after accounting for collinearity, we used the least absolute shrinkage and selection operator (LASSO) to the multiple linear regression model. We adjusted the LASSO penalty coefficients to limit to 10 input variables with nonzero linear weights. We used the coefficient of determination, r^2, as a measure of goodness-of-fit. The coefficient of determination is the proportion of variation in the output variable explained by the input variable. Values range from 0 to 1, with higher values corresponding to a better fit to the data.

Data Availability

The data used in this study will be made available on reasonable request following MCSA and ADRC study procedures.

Results

Extracted Study Cohort

Based on our inclusion criteria, we assembled a total study cohort of 223 participants (180 participants were included from MCSA and 43 participants from the ADRC database), with an average age of 77.55 (SD 8.39) years, and 57.0% (127 of 223) were male. Among these 223 participants, 119 were CU, 56 participants were diagnosed with MCI, and 48 had dementia (2 with AD dementia and 3 with Lewy body dementia). Both MCSA and ADRC study participants undergo similar imaging protocols, clinical diagnosis criteria, and quality control procedures. A detailed cohort characteristic description can be found in Table 1, where continuous variables are represented as mean and SD and count for the categorical variables.

WM NDI Negatively Correlated With Flortaucipir SUVRs in Braak Staging Regions

Based on the partial Pearson correlation analyses, only a subset of 29 WM tracts showed significant correlations ($p < 0.05$) with flortaucipir SUVR. NDI in 10 WM tracts was significantly and negatively correlated with tau deposition in Braak I region. Seventeen WM tracts were negatively correlated with flortaucipir SUVRs in Braak III/IV and Braak V/VI regions. We focused only on these WM tracts with significant correlation coefficients for the rest of this paper. The negative correlation between WM NDI and tau deposition describes an anticipated trend—higher tau deposition leads to a lower fraction of axons in the WM bundle.

Figure 3 Flortaucipir SUVRs at 3 Braak Regions
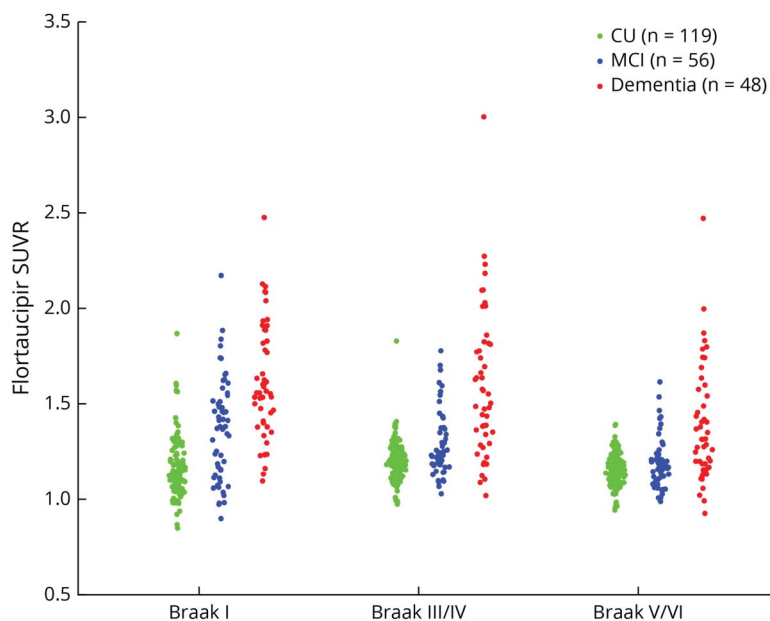
The group-level difference in between the dementia group and the other 2 groups are distinctive in Braak III/IV and V/VI regions. However, the difference between CU and MCI groups is less in Braak III–VI. The specific regions included in each Braak region can be found in eTable 2 (links.lww.com/WNL/C743). CU = cognitively unimpaired; MCI = mild cognitive impairment; SUVR = standard uptake value ratio.

Table 1 Characteristics of the Study Cohort

| Characteristic | MCSA (n = 180) | | ADRC (n = 43) |
	Cognitively unimpaired (n = 119)	Cognitively impaired (n = 61)	
Demographics and cognition			
Age, y	75.81 (8.66)	81.56 (7.50)	74.05 (6.08)
Males, %	56%	54%	63%
APOE ε4, %	39%	51%	74%
Education, y	15.11 (2.74)	13.98 (3.14)	15.70 (6.08)
MMSE	28.84 (1.07)	24.66 (3.92)	21.74 (5.15)
Clinical dementia rating scale	0.01 (0.09)	0.43 (0.34)	0.28 (0.41)
Vascular markers			
Diabetes, %	18%	23%	9%
Hypertension, %	67%	82%	51%
Hypercholesterol, %	83%	84%	42%
AD markers			
PiB SUVR	1.87 (0.38)	2.39 (0.59)	2.39 (0.43)
Tau SUVR	1.24 (0.13)	1.37 (0.23)	1.79 (0.46)

Abbreviations: AD = Alzheimer disease; ADRC = Alzheimer's Disease Research Center; MCSA = Mayo Clinic Study of Aging; MMSE = Mini-Mental State Examination; PiB = Pittsburgh compound B; SUVR = standard uptake value ratio; WM = white matter.
Demographics, cognition, vascular markers, and AD markers from 2 studies were shown: Mayo ADRC and MCSA.

Table 2 Correlation Coefficients Between Each WM NDI ROIs and Tau Deposition in Braak Stages and MMSE

| WM ROI	Braak I ($p < 0.05$)	Braak III/IV ($p < 0.05$)	Braak V/VI ($p < 0.05$)	MMSE ($p < 0.001$)
Uncinate fasciculus	−0.27	−0.31	−0.29	0.31
Cingulum adjoining hippocampus	−0.27	−0.29	−0.23	0.32
Hippocampus	−0.23	−0.23	−0.21	NS
Inferior fronto-occipital fasciculus	−0.22	−0.26	−0.24	0.29
Inferior temporal WM	−0.20	−0.28	−0.25	0.29
Middle temporal WM	−0.19	−0.28	−0.25	0.36
Superior temporal WM	−0.17	−0.23	−0.23	0.31
Cingulum	−0.15	−0.19	−0.17	0.32
Inferior occipital WM	−0.14	−0.24	−0.22	0.33
Lateral fronto-orbital WM	−0.14	−0.14	−0.15	NS
Angular WM	NS	−0.14	−0.15	NS
External capsule	NS	−0.16	−0.18	0.26
Fornix	NS	−0.15	−0.15	NS
Rectus WM	NS	−0.14	−0.14	NS
Splenium of corpus callosum	NS	−0.17	−0.16	0.30
Superior fronto-occipital fasciculus	NS	−0.14	−0.17	0.32
Supramarginal WM	NS	−0.15	−0.16	0.27

Abbreviations: NS = non-significant; MMSE = Mini-Mental State Examination; NDI = neurite density index; ROI = region of interest; WM = white matter.
The full list of the ROIs and their Braak assignment can be found in eTable 1 (links.lww.com/WNL/C742).

Specifically, the uncinate fasciculus (UNC, $r = −0.274$ for Braak I, −0.311 for Braak III/IV, and −0.292 for Braak V/VI), cingulum adjoining hippocampus (CGH, $r = −0.274$, −0.288, −0.233), and inferior fronto-occipital fasciculus (IFO, $r = −0.221$, −0.258, −0.242) ranked consistently in the top 5 WM tracts based on their associations with flortaucipir SUVRs in all 3 Braak regions. Hippocampus emerged in the top 5 WM tracts only for Braak I regions but not in later Braak regions. On the contrary, middle temporal WM (MTWM) and inferior temporal WM (ITWM) showed strong correlations with Braak III/IV and Braak V/VI regions, but not with Braak I regions. A detailed correlation coefficient rank of each WM NDI to flortaucipir SUVRs in 3 Braak regions can be found in Figure 2, B and C, where each WM tract is represented as a triangle symbol, with its correlation coefficients to all 3 Braak stage SUVRs illustrated by the height of each corner. To account for the effect of vascular disease on WM health, we also conducted a sensitivity analysis using systemic vascular risk conditions as an additional covariate. In this analysis, the associations between tau deposition and WM NDI were similar. The order of correlation significance of the WM tracts of interest remains the same as well, suggesting that vascular disease does not significantly alter our study findings.

Another line of evidence that supports the association between WM NDI and tau burden can be deduced based on the variance explained from the multiple linear regression models with 29 WM NDI as the input variables and Braak flortaucipir SUVRs as outcomes. These 29 WM NDIs accounted for 30.15% variance of the flortaucipir SUVR in Braak I region, 27.80% to flortaucipir SUVRs in Braak III/IV regions, and 19.92% to Braak V/VI regions, respectively. Moreover, when the input parameters were reduced from 29 to 10 most contributing and independent NDIs selected by LASSO, the regression model still explained 15.02% variance of Braak I flortaucipir SUVR, 17.67% to Braak III/IV flortaucipir SUVR, and 13.70% to Braak V/VI flortaucipir SUVR.

WM Tracts Affected by Tau Contribute to Lower Cognitive Performance

Because tau deposition was shown to be closely correlated with cognitive impairment and we found associations between WM integrity and tau deposition, we extended our investigation to

Figure 4 Correlation Coefficient Between WM NDI and MMSE
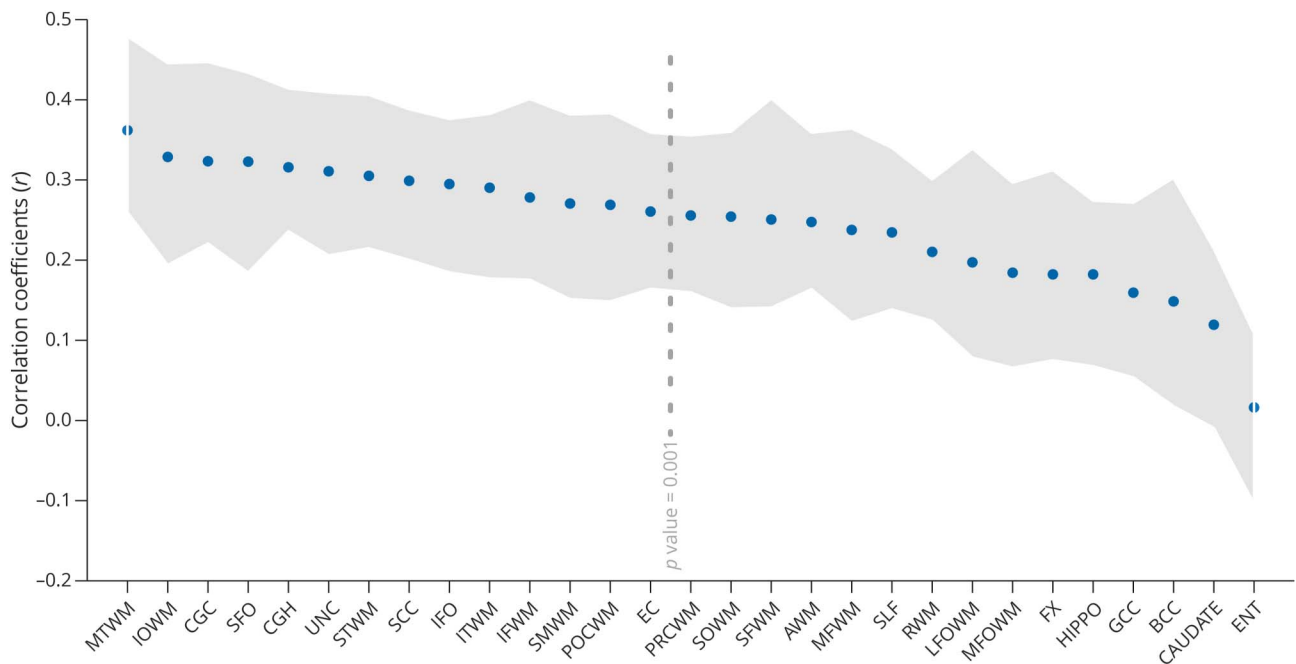
Gray area represents 95% CI. The threshold for statistical significance was set at p value = 0.001. The full list of the ROIs and their abbreviation definition can be found in eTable 1 (links.lww.com/WNL/C742). AWM = angular WM; BCC = body of corpus callosum; CAUDATE = caudate nucleus; CGC = cingulum; CGH = cingulum adjoining hippocampus; EC = external capsule; ENT = entorhinal area; FX = fornix; Hippo = hippocampus; IFO = inferior fronto-occipital fasciculus; IOWM = inferior occipital WM; ITWM = inferior temporal WM; LFOWM = lateral fronto-orbital WM; MFOWM = middle fronto-oribital WM; MFWM = middle frontal WM; MMSE = Mini-Mental State Examination; MTWM = middle temporal WM; NDI = neurite density index; POCWM = postcentral WM; PRCWM = precentral WM; RWM = rectus WM; SCC = splenium of corpus callosum; SFO = superior fronto-occipital fasciculus; SFWM = superior frontal WM; SLF = superior longitudinal fasciculus; SMWM = supramarginal WM; SOWM = superior occipital WM; STWM = superior temporal WM; UNC = uncinate fasciculus; WM = white matter.

evaluate the association between WM NDI and cognitive performance. Of 29 WM tracts, only 12 ROIs showed significant correlations ($p < 0.001$) with MMSE score (Table 2). There were positive correlations between WM NDI and MMSE performance as expected—a greater fraction of tissue in the axons, that is, less axonal damage, contributed to better cognitive performance.

The ROIs that showed the highest correlation to MMSE were the MTWM ($r = 0.362$), inferior occipital WM ($r = 0.328$), CGH ($r = 0.323$), superior fronto-occipital fasciculus ($r = 0.322$), and cingulum ($r = 0.315$). Figure 4 shows all significant correlation coefficients between WM NDI and MMSE.

Information Provided by WM NDI Comparable With Flortaucipir PET for the Describing Cognitive Performance

The effectiveness of NDI in capturing variability in cognitive performance being similar to flortaucipir PET has several implications. Therefore, we investigated the association of NDI and tau SUVR to MMSE through multiple regression models.

Regression with 29 WM NDI measures to MMSE achieved a coefficient of determination (r^2) of 31% while flortaucipir SUVRs extracted from 3 Braak regions provided a coefficient of determination of 29%. When both Braak flortaucipir SUVRs and

WM NDIs (i.e., 29 NDI and 3 Braak flortaucipir SUVR as the input variable) were combined to regress to MMSE through linear regression models, the combined model reached a coefficient of determination of 46%. This observation indicated that NDI could provide equivalent amount of information about cognition as provided by tau PET when SUVR is measured in the Braak regions. In addition, the information captured by NDI and tau deposition in describing cognitive performance was complementary and nonoverlapping because there was an increase in the coefficient of determination when both sets of measurements were combined.

Discussion

We investigated the associations between tau burden and WM damage as measured by NDI on cognitive performance. The main conclusions were (1) there was significant spatially dependent WM degeneration associated with regional tau deposition extracted from regions featured in Braak staging model. (2) NDI from these WM tracts may aid in the description of Braak stages and clinical disease stages through the association of cognitive performance. (3) Worsening WM NDI derived from NODDI provides complementary and nonoverlapping information to flortaucipir PET scans and highlights multiple pathways through which AD pathology contributes to cognitive dysfunction. (4) WM diffusion changes using dMRI could be a

useful alternative imaging approach for assessing AD-related damage and staging of the disease.

There is widespread evidence that tau aggregation is strongly correlated with cognitive impairment.[31-33] Flortaucipir PET has been shown to map well to the gold standard of pathology,[34] capture disease progression,[35,36] and is predictive of clinical disease progression.[28,37-39] Tau deposition measured by flortaucipir PET in the Braak I regions has also been shown to be associated with a lower cognition.[40]

Recent literature suggests that WM integrity in AD may be more correlated with tau than with Aβ protein.[9,41] However, the dynamics of WM changes as a function of tau deposition may be complicated. Animal models and computational models suggested that tau protein propagates through structural connectivity which could either be by trans-synaptic passage of altered tau protein or by altered synaptic homeostasis without actual physical passage of a damaged tau molecule.[42] Healthy WM tracts are the pathways through which tauopathy is propagated through anatomically connected brain regions.[43] However higher local tau accumulation may also be detrimental to the health of WM tracts.[44] A vivid analogy can be found between cars/highways and tau/WM connectivity—a wide and smooth highway enables faster traffic and may also attract higher traffic load; meanwhile, a high traffic load also increases the road's deterioration rate and eventually cause the entry pathways to break down. In this work, we focused on studying the relationships between WM tract health as a function of flortaucipir SUVRs in Braak regions with the hypothesis that the spatiotemporal progression of tau in the typical AD continuum, where tau is believed to first appear in the entorhinal cortex located in the medial temporal lobe and eventually observed throughout the entire isocortex, will be reflected in progressive deterioration of WM. Understanding these relationships has important implications not only for evaluating disease progression but also for understanding the mechanisms through which AD pathology contributes to cognitive decline and dementia.

We found that decline in WM integrity measured by NDI was associated with increased tau deposition in AD, particularly in the regions implicated in histopathologic staging.[16,35] Our findings extend the previous DTI and NODDI studies that demonstrated the association between WM degeneration and tau pathology[8,9,11,15] and further demonstrated the progressive involvement of different WM structures as disease progresses out of the medial temporal lobe.

The most significant negative association between WM NDI and tau deposition in Braak staging I and III/IV was found in UNC and CGH. UNC is traditionally considered a part of the limbic cortex, connects the limbic structures in the medial temporal region to the frontal lobes (i.e., a direct bridge between early and late Braak regions), and plays an important role in episodic memory. The UNC was found to be the most consistent tract affected by tau deposition in Braak I–VI, and

this finding is supported by UNC's anatomical proximity to regions of early tau deposition and its key role in the limbic system. Future work will benefit from investigating the causal pathways through which UNC may play a role in early stages of AD. The effect of tau in Braak I and III/IV regions was also observed on CGH WM, which is the most studied tract for tau propagation in AD and connects the medial temporal lobe to the posterior cingulate cortex.[8,45] Given that posterior cingulate cortex is a major cortical hub with widespread connectivity to the entire brain,[46] CGH WM's key role in tau accumulation outside the medial temporal lobe has been confirmed by our findings. Hippocampal WM tract had stronger associations with Braak I flortaucipir SUVR as opposed to III-VI as expected because of anatomical proximity.

As the extent of AD pathology moves out from Braak I to Braak III–VI, WM disconnectivity in the temporal lobes (MTWM and ITWM) showed strong correlations with flortaucipir SUVRs. Inferior temporal cortex has been implicated as a core region for tau pathology.[37] Previous studies have shown synaptic loss[47] and regional cortical thinning[48] in the inferior temporal gyrus in MCI and AD dementia. Our current work further emphasized the connectivity in inferior, middle, and to some extent, superior temporal regions as important. Consistent with our findings, a previous study demonstrated a negative correlation between tau PET tracer (18F-THK5351) and NDI in the bilateral lateral and medial temporal lobes, suggesting tau and neuroinflammation as the possible cause of reduced NDI in amyloid-positive participants.[14] In addition, in line with the Braak staging, Wen et al.[15] assessed the relationship between GM tau-PET signal and WM microstructure using NODDI and found most significant spatial association patterns originated from medial temporal lobe and then extended into posterior occipital and parietal regions and then to frontal lobes.

Our study provides strong evidence that subtle WM microstructural changes because of increasing tau deposition cannot be discounted and significantly contributes to cognitive impairment. The increased explained variance by both tau and WM feature indicates that the underlying mechanism for cognitive impairment in AD is multifactorial. Most of the AD research so far has been focused on the degree of tau deposition and the resulting GM damage from tau. However, it is noteworthy that cognitive impairment is due to the cumulative consequence of multiple factors, such as Aβ, tau, loss of neurons and synapses, axonal degradation, etc. Therefore, identifying multiple mechanisms and measuring these to map the causal evolution of disease processes is critical.

dMRI is accessible, noninvasive, and is often acquired as part of routine MRI, often a part of participant screening for clinical trials and research studies. Modern MRI scanners are increasingly equipped with multiband capability, enabling them to capture advanced dMRI images needed for the generation of NDI from NODDI without hardware modifications. Based on the results shown in this work, NDI

provides information about AD disease progression and stage and may be an invaluable clinical tool in early-stage AD.

This study has some strengths and limitations. A major strength is the availability of advanced dMRI, flortaucipir-PET, and cognitive scores in 2 well-characterized samples covering the AD continuum. Although there was limited availability of longitudinal data to investigate the temporal dynamics between NDI and tau progression, we used Braak staging as a template model for describing the tau deposition progression in typical AD. Another weakness is that we considered Braak staging to be a rather coarse description model for tau deposition in typical AD. The deviation from this typical progression of tau (seen in >60% of individuals) is widely recognized. Given the measurements of regional tau, we considered that there are remaining variances in cognition that can be explained by WM. It is possible that better tau assessment methods (imaging acquisition/ processing/inclusion of more regions) could further explain the stronger association contributed by WM. Still, the simplistic approach we took allowed us to deduce the WM involvement more clearly.[49] For the statistical analyses, we also considered the weakness could be found in the number of statistical tests included in this study. A large number of statistical tests will likely lead to a high risk of type I error. However, given the exploratory nature of this study and the interest in individual regions and tracts as opposed to a universal hypothesis, we did not choose to reduce that probability while increasing the probability of a type II error through a smaller significance cutoff or multiple comparison adjustment.[50] Validation of the results through future studies will be required to confirm these findings. In addition, the samples in this study were convenience samples, and we did not provide power calculation. Given the number of different tests and because each set of circumstances would require a new calculation, power calculations were not feasible at the current phase.

Future work will focus on the temporal dynamics using multimodal biomarkers that capture distinctive properties in various phases of the disease.

Acknowledgment

Study Funding

Disclosure

Publication History

Appendix Authors

Name	Location	Contribution
Jianqiao Tian, MS	Department of Radiology, Mayo Clinic; Mayo Clinic Graduate School of Biomedical Sciences, Rochester, MN	Drafting/revision of the manuscript for content, including medical writing for content; study concept or design; analysis or interpretation of data
Sheelakumari Raghavan, PhD	Department of Radiology, Mayo Clinic, Rochester, MN	Drafting/revision of the manuscript for content, including medical writing for content; study concept or design; analysis or interpretation of data
Robert I. Reid, PhD	Department of Information Technology, Mayo Clinic, Rochester, MN	Drafting/revision of the manuscript for content, including medical writing for content; analysis or interpretation of data
Scott A. Przybelski, BS	Department of Quantitative Health Sciences, Mayo Clinic, Rochester, MN	Drafting/revision of the manuscript for content, including medical writing for content; analysis or interpretation of data
Timothy G. Lesnick, MS	Department of Quantitative Health Sciences, Mayo Clinic, Rochester, MN	Drafting/revision of the manuscript for content, including medical writing for content; analysis or interpretation of data
Robel K. Gebre, PhD	Department of Radiology, Mayo Clinic, Rochester, MN	Drafting/revision of the manuscript for content, including medical writing for content; analysis or interpretation of data
Jonathan Graff-Radford, MD	Department of Neurology, Mayo Clinic, Rochester, MN	Drafting/revision of the manuscript for content, including medical writing for content
Christopher G. Schwarz, PhD	Department of Radiology, Mayo Clinic, Rochester, MN	Drafting/revision of the manuscript for content, including medical writing for content

Continued

Appendix (continued)

Name	Location	Contribution
Val J. Lowe, MD	Department of Radiology, Mayo Clinic, Rochester, MN	Drafting/revision of the manuscript for content, including medical writing for content; major role in the acquisition of data
Kejal Kantarci, MD	Department of Radiology, Mayo Clinic, Rochester, MN	Drafting/revision of the manuscript for content, including medical writing for content
David S. Knopman, MD	Department of Neurology, Mayo Clinic, Rochester, MN	Drafting/revision of the manuscript for content, including medical writing for content; major role in the acquisition of data
Ronald C. Petersen, MD, PhD	Department of Neurology, Mayo Clinic, Rochester, MN	Drafting/revision of the manuscript for content, including medical writing for content; major role in the acquisition of data
Clifford R. Jack, Jr., MD	Department of Radiology, Mayo Clinic, Rochester, MN	Drafting/revision of the manuscript for content, including medical writing for content; major role in the acquisition of data
Prashanthi Vemuri, PhD	Department of Radiology, Mayo Clinic, Rochester, MN	Drafting/revision of the manuscript for content, including medical writing for content; major role in the acquisition of data; study concept or design; analysis or interpretation of data

References

1. Madden DJ, Bennett IJ, Song AW. Cerebral white matter integrity and cognitive aging: contributions from diffusion tensor imaging. *Neuropsychol Rev.* 2009;19(4):415-435. doi:10.1007/s11065-009-9113-2
2. Agosta F, Weiler M, Filippi M. Propagation of pathology through brain networks in neurodegenerative diseases: from molecules to clinical phenotypes. *CNS Neurosci Ther.* 2015;21(10):754-767.
3. Mito R, Raffelt D, Dhollander T, et al. Fibre-specific white matter reductions in Alzheimer's disease and mild cognitive impairment. *Brain.* 2018;141(3):888-902.
4. Dewenter A, Jacob MA, Cai M, et al. Disentangling the effects of Alzheimer's and small vessel disease on white matter fibre tracts. *Brain.* 2023;146(2):678-689.
5. Zhang H, Schneider T, Wheeler-Kingshott CA, Alexander DC. NODDI: practical in vivo neurite orientation dispersion and density imaging of the human brain. *Neuroimage.* 2012;61(4):1000-1016.
6. McAleese KE, Walker L, Graham S, et al. Parietal white matter lesions in Alzheimer's disease are associated with cortical neurodegenerative pathology, but not with small vessel disease. *Acta Neuropathol.* 2017;134(3):459-473.
7. Kantarci K, Murray ME, Schwarz CG, et al. White-matter integrity on DTI and the pathologic staging of Alzheimer's disease. *Neurobiol Aging.* 2017;56:172-179.
8. Jacobs HIL, Hedden T, Schultz AP, et al. Structural tract alterations predict downstream tau accumulation in amyloid-positive older individuals. *Nat Neurosci.* 2018;21(3):424-431.
9. Strain JF, Smith RX, Beaumont H, et al. Loss of white matter integrity reflects tau accumulation in Alzheimer disease defined regions. *Neurology.* 2018;91(4):e313-e318.
10. Sintini I, Schwarz CG, Martin PR, et al. Regional multimodal relationships between tau, hypometabolism, atrophy, and fractional anisotropy in atypical Alzheimer's disease. *Hum Brain Mapp.* 2019;40(5):1618-1631.
11. Hall Z, Chien B, Zhao Y, et al. Tau deposition and structural connectivity demonstrate differential association patterns with neurocognitive tests. *Brain Imaging Behav.* 2022;16(2):702-714.
12. Colgan N, Siow B, O'Callaghan JM, et al. Application of neurite orientation dispersion and density imaging (NODDI) to a tau pathology model of Alzheimer's disease. *Neuroimage.* 2016;125:739-744.
13. Anderson JAE, Schifani C, Nazeri A, Voineskos AN. In vivo cortical microstructure: a proxy for tauopathy and cognitive impairment in the elderly with and without MCI/dementia. *meRxiv.* 2021. doi:10.1101/2021.03.26.21254351
14. Sone D, Shigemoto Y, Ogawa M, et al. Association between neurite metrics and tau/inflammatory pathology in Alzheimer's disease. *Alzheimers Dement (Amst).* 2020;12(1):e12125.
15. Wen Q, Risacher SL, Xie L, et al. Tau-related white-matter alterations along spatially selective pathways. *Neuroimage.* 2021;226:117560.
16. Braak H, Braak E. Neuropathological stageing of Alzheimer-related changes. *Acta Neuropathol.* 1991;82(4):239-259.
17. Lowe VJ, Wiste HJ, Senjem ML, et al. Widespread brain tau and its association with ageing, Braak stage and Alzheimer's dementia. *Brain.* 2017;141(1):271-287.
18. Roberts RO, Geda YE, Knopman DS, et al. The Mayo Clinic Study of Aging: design and sampling, participation, baseline measures and sample characteristics. *Neuroepidemiology.* 2008;30(1):58-69.
19. Rocca WA, Yawn BP, St Sauver JL, Grossardt BR, Melton LJ III. History of the Rochester Epidemiology Project: half a century of medical records linkage in a US population. *Mayo Clin Proc.* 2012;87(12):1202-1213.
20. Petersen RC, Roberts RO, Knopman DS, et al. Prevalence of mild cognitive impairment is higher in men. The Mayo Clinic Study of Aging. *Neurology.* 2010;75(10):889-897.
21. Raghavan S, Reid RI, Przybelski SA, et al. Diffusion models reveal white matter microstructural changes with ageing, pathology and cognition. *Brain Commun.* 2021;3(2):fcab106.
22. Veraart J, Novikov DS, Christiaens D, Ades-Aron B, Sijbers J, Fieremans E. Denoising of diffusion MRI using random matrix theory. *Neuroimage.* 2016;142:394-406.
23. Andersson JLR, Sotiropoulos SN. An integrated approach to correction for off-resonance effects and subject movement in diffusion MR imaging. *Neuroimage.* 2016;125:1063-1078.
24. Kellner E, Dhital B, Kiselev VG, Reisert M. Gibbs-ringing artifact removal based on local subvoxel-shifts. *Magn Reson Med.* 2016;76(5):1574-1581.
25. Koay CG, Ozarslan E, Basser PJ. A signal transformational framework for breaking the noise floor and its applications in MRI. *J Magn Reson.* 2009;197(2):108-119.
26. Daducci A, Canales-Rodríguez EJ, Zhang H, Dyrby TB, Alexander DC, Thiran JP. Accelerated Microstructure Imaging via Convex Optimization (AMICO) from diffusion MRI data. *Neuroimage.* 2015;105:32-44.
27. Oishi K, Faria A, Jiang H, et al. Atlas-based whole brain white matter analysis using large deformation diffeomorphic metric mapping: application to normal elderly and Alzheimer's disease participants. *Neuroimage.* 2009;46(2):486-499.
28. Jack CR Jr, Wiste HJ, Weigand SD, et al. Defining imaging biomarker cut points for brain aging and Alzheimer's disease. *Alzheimers Dement.* 2017;13(3):205-216.
29. Baker SL, Maass A, Jagust WJ. Considerations and code for partial volume correcting [(18)F]-AV-1451 tau PET data. *Data Brief.* 2017;15:648-657.
30. Kokmen E, Smith GE, Petersen RC, Tangalos E, Ivnik RC. The short test of mental status: correlations with standardized psychometric testing. *Arch Neurol.* 1991;48(7):725-728.
31. Xia C, Makaretz SJ, Caso C, et al. Association of in vivo [18F]AV-1451 tau PET imaging results with cortical atrophy and symptoms in typical and atypical Alzheimer disease. *JAMA Neurol.* 2017;74(4):427-436.
32. Bejanin A, Schonhaut DR, La Joie R, et al. Tau pathology and neurodegeneration contribute to cognitive impairment in Alzheimer's disease. *Brain.* 2017;140(12):3286-3300.
33. Jack CR Jr, Knopman DS, Jagust WJ, et al. Tracking pathophysiological processes in Alzheimer's disease: an updated hypothetical model of dynamic biomarkers. *Lancet Neurol.* 2013;12(2):207-216.
34. Lowe VJ, Lundt ES, Albertson SM, et al. Tau-positron emission tomography correlates with neuropathology findings. *Alzheimers Dement.* 2020;16(3):561-571.
35. Schöll M, Lockhart SN, Schonhaut DR, et al. PET imaging of tau deposition in the aging human brain. *Neuron.* 2016;89(5):971-982.
36. Schwarz AJ, Shcherbinin S, Slieker LJ, et al. Topographic staging of tau positron emission tomography images. *Alzheimers Dement (Amst).* 2018;10(1):221-231.
37. Johnson KA, Schultz A, Betensky RA, et al. Tau positron emission tomographic imaging in aging and early Alzheimer disease. *Ann Neurol.* 2016;79(1):110-119.
38. Jack CR Jr, Knopman DS, Jagust WJ, et al. Hypothetical model of dynamic biomarkers of the Alzheimer's pathological cascade. *Lancet Neurol.* 2010;9(1):119-128.
39. Bucci M, Chiotis K, Nordberg A. Alzheimer's disease profiled by fluid and imaging markers: tau PET best predicts cognitive decline. *Mol Psychiatry.* 2021;26(10):5888-5898.
40. Knopman DS, Lundt ES, Therneau TM, et al. Entorhinal cortex tau, amyloid-β, cortical thickness and memory performance in non-demented subjects. *Brain.* 2019;142(4):1148-1160.
41. Pereira JB, Ossenkoppele R, Palmqvist S, et al. Amyloid and tau accumulate across distinct spatial networks and are differentially associated with brain connectivity. *Elife.* 2019;8:e50830.
42. Vogel JW, Iturria-Medina Y, Strandberg OT, et al. Spread of pathological tau proteins through communicating neurons in human Alzheimer's disease. *Nat Commun.* 2020;11(1):2612.
43. Mudher A, Colin M, Dujardin S, et al. What is the evidence that tau pathology spreads through prion-like propagation? *Acta Neuropathol Commun.* 2017;5(1):99.
44. Iqbal K, Liu F, Gong C-X, Alonso AdC, Grundke-Iqbal I. Mechanisms of tau-induced neurodegeneration. *Acta Neuropathol.* 2009;118(1):53-69.
45. Pichet Binette A, Theaud G, Rheault F, et al. Bundle-specific associations between white matter microstructure and Aβ and tau pathology in preclinical Alzheimer's disease. *Elife.* 2021;10:e62929.
46. Leech R, Braga R, Sharp DJ. Echoes of the brain within the posterior cingulate cortex. *J Neurosci.* 2012;32(1):215-222.
47. Scheff SW, Price DA, Schmitt FA, Scheff MA, Mufson EJ. Synaptic loss in the inferior temporal gyrus in mild cognitive impairment and Alzheimer's disease. *J Alzheimers Dis.* 2011;24(3):547-557.
48. Bakkour A, Morris JC, Dickerson BC. The cortical signature of prodromal AD: regional thinning predicts mild AD dementia. *Neurology.* 2009;72(12):1048-1055.
49. Vogel JW, Young AL, Oxtoby NP, et al. Four distinct trajectories of tau deposition identified in Alzheimer's disease. *Nat Med.* 2021;27(5):871-881.
50. Rothman KJ. No adjustments are needed for multiple comparisons. *Epidemiology.* 1990;1:43-46.